Chapter 1

Calibration

Chapter 7 Opening

1.1 Electron Lifetime

1.1.1 Measurement Procedure

1.1.2 Lifetime Correction

1.1.3 Bias Study From Diffusion and Space Charge Effects

1.1.4 Look Up Curve

1.1.5 Bias Study From Geometry of Cosmic Ray Tracks

1.1.6 Concluding Remarks

1.2 Delta Ray Fluctuations on Recombination Simulation

As discussed in Chapter **??**, simulation plays a vital role in neutrino physics. The need to correctly simulate physics processes must be addressed in order to validate against data and build towards a data-driven simulation. The physics process of this simulated study is recombination, which drives the charge and light yield. As described in Sec. **??**, the recombination model employed at SBND is an phenomenological model, with parameters that have been experimentally measured by ArgoNeuT and tuned for simulation to match data [1]. The Modified Box (ModBox) model approximates the recombination probability based on a cylindrical column surrounding a track-like charge deposition. This volume treatment effectively accounts for microphysics processes produced along the track, such as delta rays, as some additional charges of the track itself. This approximation has proven to work well for the MeV to GeV-scale interactions, energy range relevant to LArTPC detector, however, breaks down when applying to keV-scale interactions. The NEST collaboration has pointed out non-linear fluctuations in recombination at increasingly smaller scales, which is currently not well-described by the ModBox model [2]. Moreover, the ArgoNeuT collaboration has also proposed that microphysics effects could lead to disagreements in recombination theory and simulation and measurement [1].

One microphysics process that can affect recombination, highlighted by both NEST and ArgoNeuT collaborations, is delta ray. Delta rays are high dE/dx knock-out electrons with energy as low as 1 keV. As shown in Fig. **??**, delta rays can be seen as short tracks pro-

duced along a longer primary track, in this case, a cosmic muon. Since delta rays have high dE/dx, they are associated with a smaller recombination factor, producing more scintillation photons while quenching ionisation electrons. This simulation investigation examines how fluctuation in delta rays impacts the recombination simulation, and consequently, the energy-charge scales of different particle types. Sec. **??** explains the simulation framework of delta rays and recombination, an expresses some concerns associated with the current simulation framework. Sec. **??**, **??** and **??** describes the impacts of varying configurable simulation handles associated with delta rays on particle calorimetry. Finally, Sec. **??** suggest recommendations for future work, with a focus on data-driven approaches.

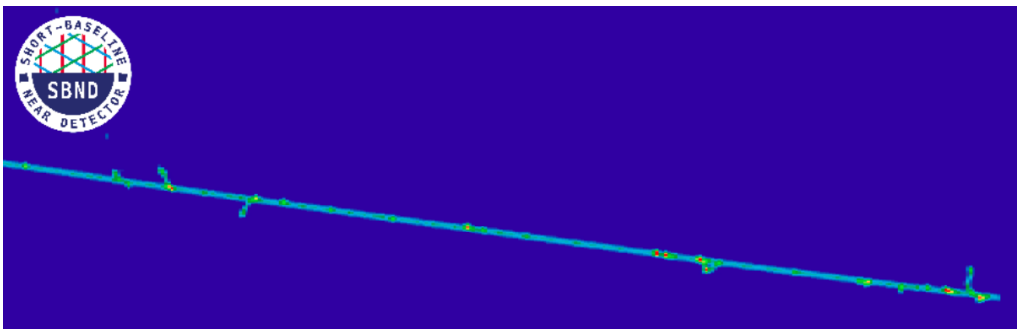

Fig. 1.1 Event display of a simulated cosmic muon track segment, with many delta rays produced along the primary track.

1.2.1 Simulation of Delta Rays and Recombination

The physics of particle propagation from creation to detection point is simulated at the LArG4 stage as described in Chapter **??**. This stage is responsible to propagate the primary particle step by step and apply physics processes to each step of length dx. LArG4 simulates the physics of energy loss due to ionisation as two intertwined processes: (1) a continuous energy loss dE of the primary particle along the step dx and (2) a discrete energy loss at the end of the step to produce delta rays. The distribution of energy deposition per step dE/dx is defined by an energy threshold. For the continuous energy loss process, the energy threshold restricts the upper limit of the stopping power so that the mean energy loss is less than the threshold. For the delta ray production process, the energy threshold defines the lower limit of the kinetic energy of the generated delta rays. In other words, the energy threshold determines how much energy deposition is shared between the primary particle and the delta rays. The lower the threshold, the more energy deposition is carried away by the delta rays instead of the primary particle.

In LArG4 terminology, this energy threshold is also known as the secondary production threshold, where the minimum kinetic energy requirement for delta ray production is defined as the minimum distance the generated delta ray must be able to traverse in a given material. For the standard simulation in SBND, the secondary production threshold for delta rays in a LAr medium is set as 700 μm, equivalent to delta ray having a kinetic energy of 273 keV. Moreover, the maximum length dx that the particle can propagate per step is set as 0.3 mm. This setup allows for a more feasible computation by not generating and tracking all possible low energy delta rays.

Recombination is then simulated for each step to determine the charge and light yield. SBND employs the ModBox model, describing the energy-charge scale as follow

$$\frac{dE}{dx} = \frac{1}{\beta}\left[\exp\left(\beta W_{ion}\frac{dQ}{dx}\right) - \alpha\right] \tag{1.1}$$

where $\alpha = 0.93$ and $\beta = 0.30$ cm/MeV, which are parameters that have been experimentally derived by ArgoNeuT [1]. Recombination is highly dependent on the electric field and the local charge density, and therefore a parameter for electric field is folded into the β parameter. By re-arranging Eq. **??**, one can derive the formalism of the recombination factor R as a function of dE/dx

$$R = \frac{\log\left(\alpha + \left(\beta \cdot dE/dx\right)/\varepsilon\right)}{\left(\beta \cdot dE/dx\right)/\varepsilon} \tag{1.2}$$

where ε is the electric field of the detector at the position of the step. For each step dx, the number of electron-ion pairs is calculated by dividing the energy deposited dE by the energy required to ionise an argon atom $W_{ion} = 23.6$ eV. Then, R from in Eq. **??** is applied according to the charge-light anti-correlation previously described by Eq. **??**, to determine the final charge and light yield resulting from the step dx.

The parameters α and β of Eq. **??** were measured by ArgoNeuT using a stopping proton sample with a wire pitch of 3 mm. Thus, the simulation of delta rays and recombination can give rise to several concerns. The first concern is the assumption of a *universal* recombination factor R, where the same value is applied to different types of ionising particle which can influence the local ionisation density differently. Secondly, the secondary production threshold on delta rays remove low energy electrons in simulation, however, they are produced in reality and can fluctuate recombination at a local scale. The last concern is the step length dx configured to be one order of magnitude smaller than the wire pitch of both ArgoNeuT and SBND, resulting in the effective recombination R being applied at a microscopic scale.

The simulation investigation was set up to address individual concern as well as to better understand their impacts on recombination. A truth comparison was carried out on two identical samples of muons and protons, to investigate if recombination is particle-dependent. The particles were generated with a fixed energy of 1 GeV, uniform in positional and angular distributions. The LArG4 stage was configured such that the particle can only deposit energy via ionisation. Then, a charge-based calorimetry was performed by reconstructing deposited energy dE/dx from deposited charge dQ/dx using Eq. **??**.

1.2.2 Impacts of Delta Ray Fluctuations On Recombination Magnitude

Fluctuations in delta rays were examined at different values of the secondary production thresholds ranging from 700 μm to 1 μm. This is equivalent to generating delta rays of minimum kinetic energy ranging from 273 keV to as low as 1 keV. The energy-charge plots of dQ/dx to dE/dx for proton are shown in Fig. **??**, for the secondary production threshold at 700 μm and 1 μm. The calorimetry is plotted for the proton residual range from 1 cm to 90 cm, which covers the full track length. The proton dE/dx proton ranges from 2 MeV/cm to 18 MeV/cm, allowing for the examination of delta ray fluctuation impacts at both low and high spectrum of dE/dx. For the secondary production threshold of 700 um, the calorimetry distribution precisely follows the ModBox model with the ArgoNeuT parameters. The good agreement is expected since the standard simulation of SBND is similar to the described simulation framework by ArgoNeuT [1]: (1) the maximum step length dx was restricted to be 0.3 mm and (2) the energy loss due to delta rays was not included in recombination.

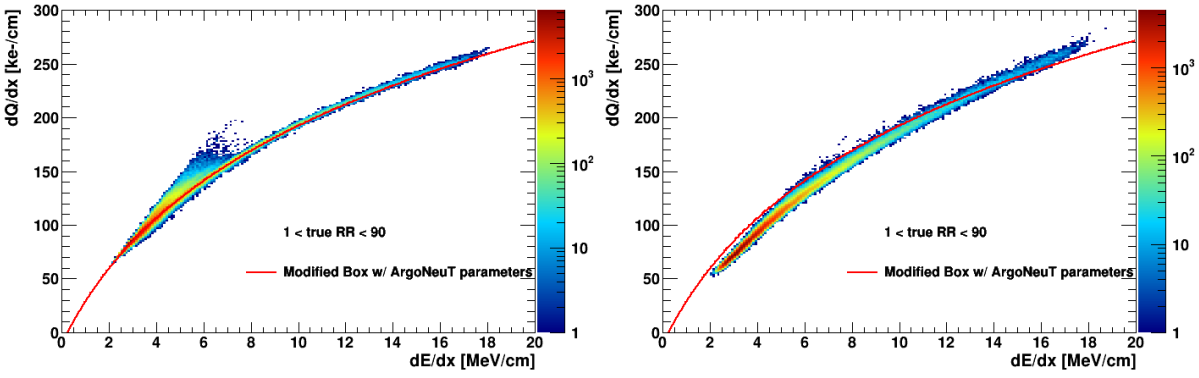

(a) Secondary production threshold at 700 μm **(b)** Secondary production threshold at 1 μm

Fig. 1.2 Plots of dQ/dx as a function of dE/dx for a 1 GeV proton at two values of secondary production threshold: 700 μm (left) and 1 μm (right)

However, for the secondary production threshold of 1 um, deviations away from the ModBox model occurs, such that the energy-charge scale shifts in opposite directions at low dE/dx compared to high dE/dx. Lowering the secondary production threshold leads to more energy deposition carried by the delta rays instead of the proton, and thus, delta rays have greater influence on recombination. At the low dE/dx spectrum of proton, delta rays have higher dE/dx than that of proton, resulting in the effective recombination factor being quenched. The opposite effect is seen at the high dE/dx spectrum of proton, resulting in the effective recombination factor increases.

The energy-charge scale of proton at the secondary production thresholds at 700, 10, 5, 1 μm, equivalent to delta rays with minimum kinetic energy of 272.58, 14.60, 2.58, 1.06 and 0.99 keV are plotted in Fig. **??**. To compare dQ/dx quantitatively at the same dE/dx bin, the mean dQ/dx is calculated per bin as shown in Fig. **??**. The percentage difference of the mean dQ/dx relative to the ModBox model are plotted in Fig. **??** to examine the magnitude of impacts from delta rays fluctuations on the energy-charge scale. Lowering the kinetic energy of delta rays results in two key trends. Firstly, the dE/dx position at which the proton energy-charge scale shifts in opposite directions, increases with lower delta ray kinetic energy. Secondly, the magnitude of the deviations is also dependent on the delta ray kinetic energy. At low dE/dx, the magnitude of the effective recombination quenching is the greatest for the secondary production threshold set as 1 μm. Meanwhile at high dE/dx, the effective recombination is the highest for the secondary production threshold set as 10 μm. This is evident that delta ray fluctuations determine how much the proton is *dressed* in

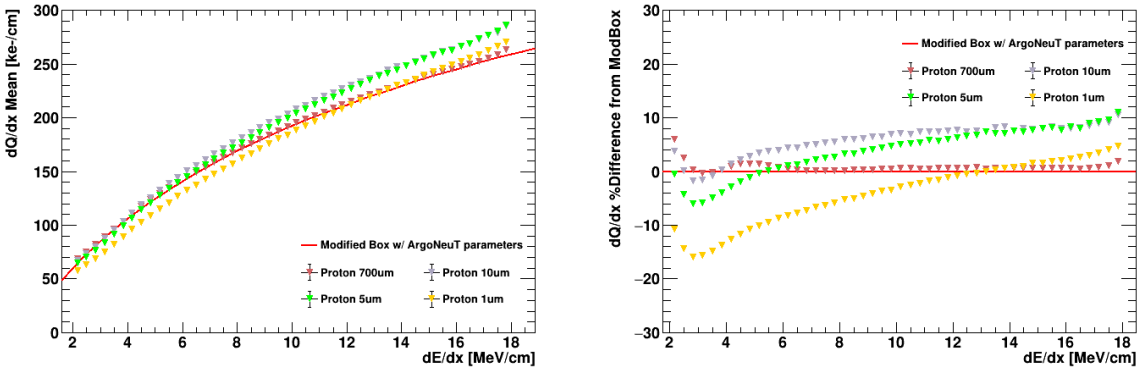

(a) **(b)**

Fig. 1.3 Plots of the mean dQ/dx (left) and its percentage difference relative to the ModBox model (right) as a function of dE/dx for a 1 GeV proton at various values of secondary production thresholds.

delta rays, and can greatly influence the effective recombination factor across the dE/dx spectrum of proton.

The calorimetry plot for muon is plotted in Fig. **??**, for the secondary production threshold at 700 μm and 1 μm respectively. Fig. **??** and **??** contain no restriction on the muon residual range is applied, to fully cover the track length from 1 to 400 cm. Two distinct distributions can be seen, one linear prong from the MIP muon region, and another one that follows curve of the ModBox model indicating the muon stopping region. The linear energy-charge scale has been well-observed experimentally with MIP muons []. In order to examine the stopping region exclusively, a residual range requirement of less than 10 cm

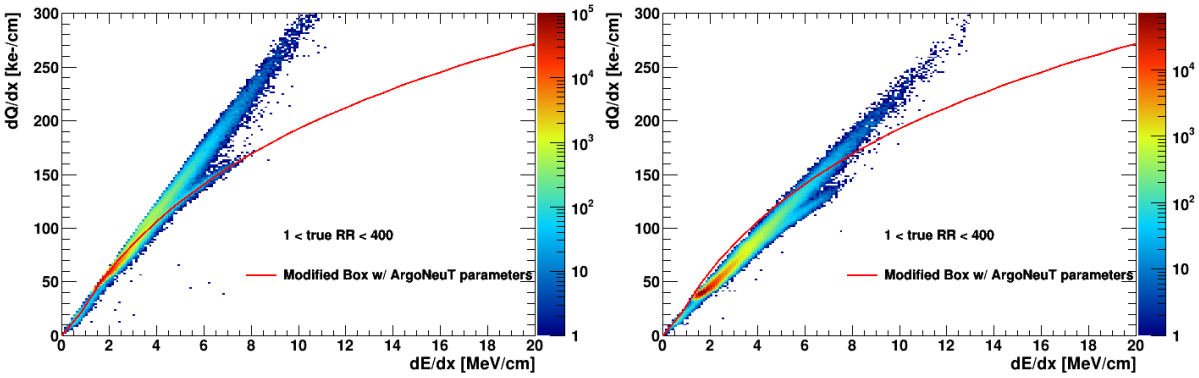

(a) Secondary production threshold at 700 μm and full residual range

(b) Secondary production threshold at 1 μm and full residual range

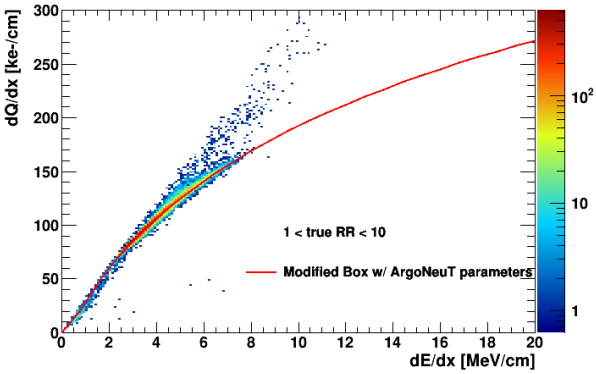

(c) Secondary production threshold at 700 μm and only stopping range

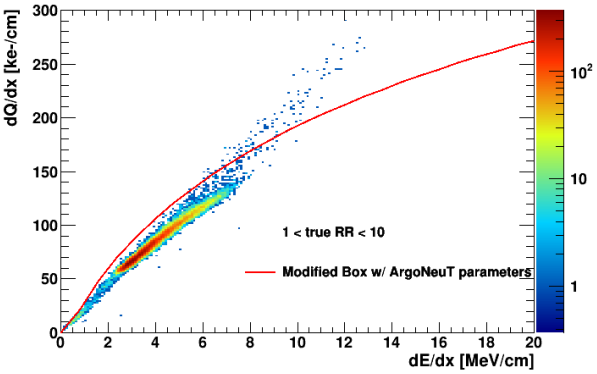

(d) Secondary production threshold at 1 μm and only stopping range

Fig. 1.4 Plots of dQ/dx as a function of dE/dx for a 1 GeV muon at two values of secondary production threshold: 700 μm (left) and 1 μm (right). Full residual range of the muon is included in the top plots and only stopping range is included in the bottom plots.

is applied, as shown Fig. **??** and **??**. Some remnants of the MIP muon distribution can still be seen in the dE/dx range between 4 to 12 MeV/cm. Similarly to proton at the low dE/dx scale, delta rays with lower kinetic energy results in quenching the effective recombination factor. The mean dQ/dx of muon and its percentage difference relative to the ModBox model are also plotted as shown in Fig. **??**. The same behaviour as proton is observed such that the magnitude of the effective recombination quenching increases with lower delta ray kinetic energy. Nonetheless, the magnitude of the quenching is larger for muon compared to proton. The difference is driven by how each particle type is *dressed* in a different amount delta rays even at the same simulation configuration for delta rays.

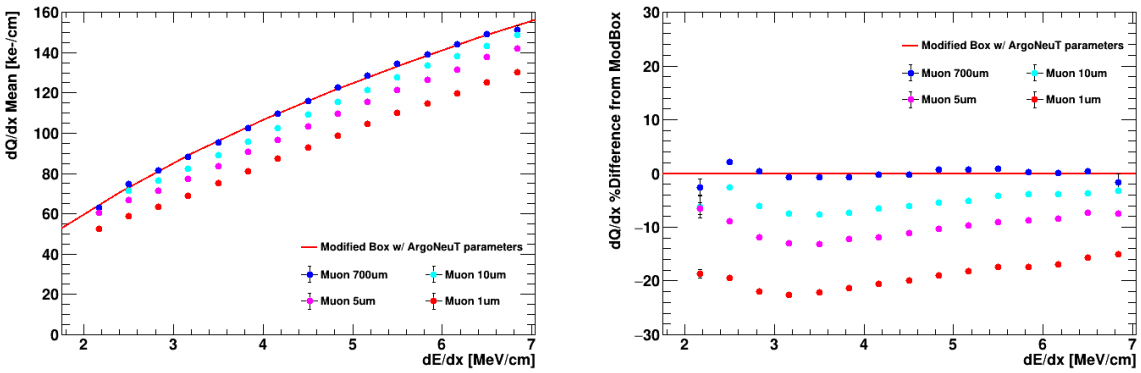

(a) **(b)**

Fig. 1.5 Plots of the mean dQ/dx (left) and its percentage difference relative to the ModBox model (right) as a function of dE/dx for a 1 GeV muon at various values of secondary production thresholds.

1.2.3 Impacts of Delta Ray Fluctuations On Recombination Smearing

The effects of delta rays on recombination also extends to smearing of the energy-charge scale. In order to de-tangle how the LArG4 simulation framework handles the smearing due delta rays, additional study was carried by isolating only the energy deposition of the primary particle. Fig. **??** shows the dE/dx of the primary proton as a function of its residual range, compared against the Landau-Vavilov distribution [] plotted in solid red line. Energy loss due to delta rays are included in the top two plots, Fig. **??** and Fig. **??**, for the secondary production thresholds of 700 μm and 1 μm. Meanwhile, the bottom two plots, Fig. **??** and Fig. **??**, only include the energy loss of the primary proton. The same set of plots are also computed for the case of muon as shown in Fig. **??**.

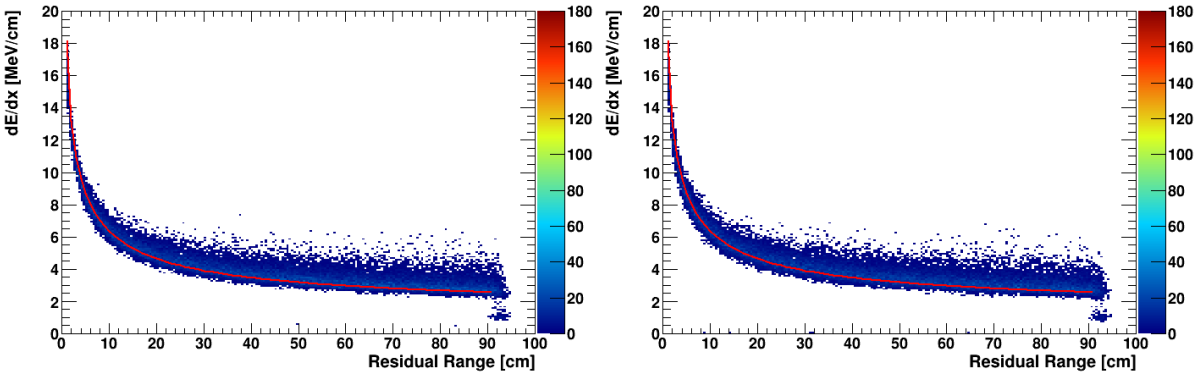

(a) Secondary production threshold at 700 μm and delta rays are included

(b) Secondary production threshold at 1 μm and delta rays are included

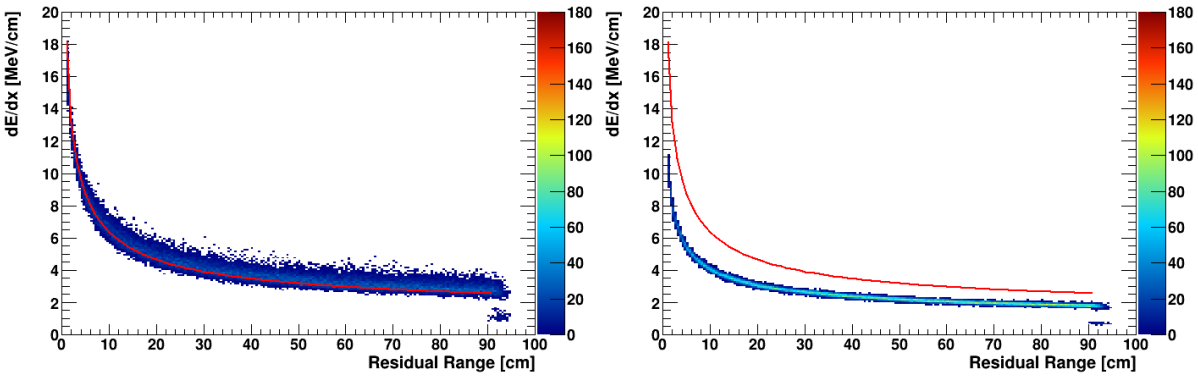

(c) Secondary production threshold at 700 μm and delta rays are excluded

(d) Secondary production threshold at 1 μm and delta rays are excluded

Fig. 1.6 Plots of dE/dx as a function of residual range for a 1 GeV proton with different secondary production thresholds at 700 μm (left) and 1 μm (right). The top and bottom plots include and exclude the energy depositions from delta rays respectively. All distributions are compared against the Landau-Vavilov distributions plotted in solid red line.

When delta rays are included in the energy deposition, the dE/dx distribution agrees with the Landau-Vavilov distribution with smearing in dE/dx across all bins of residual range. The distributions are indistinguishable between the secondary production threshold at the default secondary production threshold of 700 um and 1 um, comparing Fig. **??** and Fig. **??** for proton and comparing Fig. **??** and **??** for muon. The behaviour is expected since the total energy deposition of the primary particle, and the delta rays stay the same at different values of the secondary production threshold.

As stated previously, the secondary production threshold changes how much the energy loss is shared between the primary particle and the associated delta rays. This is evident

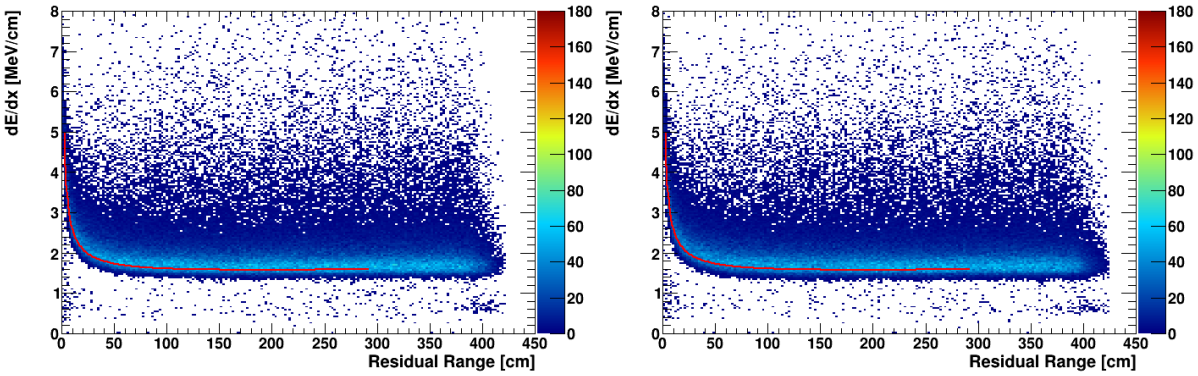

(a) Secondary production threshold at 700 μm and delta rays are included

(b) Secondary production threshold at 1 μm and delta rays are included

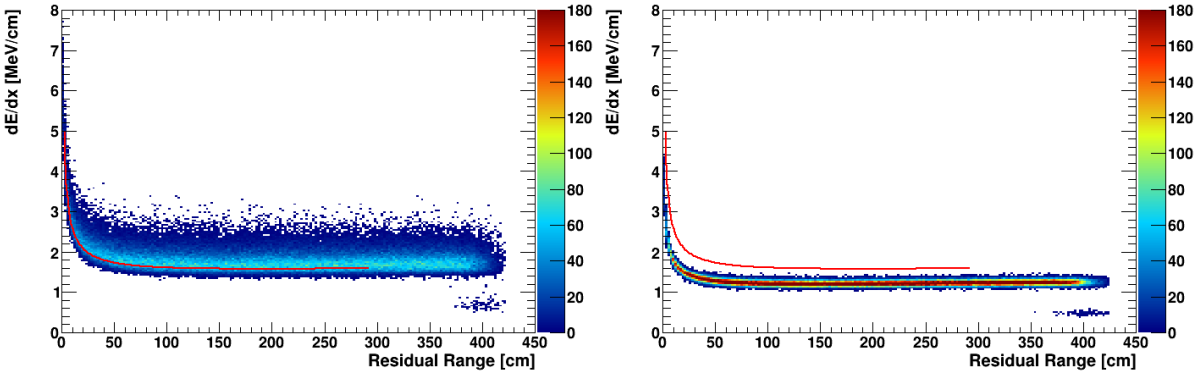

(c) Secondary production threshold at 700 μm and delta rays are excluded

(d) Secondary production threshold at 1 μm and delta rays are excluded

Fig. 1.7 Plots of dE/dx as a function of residual range for a 1 GeV muon with different secondary production thresholds at 700 μm (left) and 1 μm (right). The top and bottom plots include and exclude the energy depositions from delta rays respectively. All distributions are compared against the Landau-Vavilov distributions plotted in solid red line.

when considering only the energy deposition of from the primary particle. For the secondary production threshold of 700 μm, the dE/dx distribution of only the primary particle follows closely the Landau-Vavilov distribution, however with less smearing in dE/dx compared to when delta rays are included in the energy loss. This can be seen comparing Fig. **??** and Fig. **??** for proton, and comparing Fig. **??** and **??** for muon. Meanwhile, when the secondary production threshold is set to 1 um and no delta rays are considered, the dE/dx distribution becomes narrow without any smearing and fails to follow the Landau-Vavilov distribution, which can be seen in Fig. **??** for proton and Fig. **??** for muon.

This study provides insight into understanding how the LArG4 framework introduces smearing in the energy deposition due to fluctuations in delta rays. The smearing is applied twice when LArG4 sampling the energy loss due ionisation, which is made up of two processes: (1) a continuous energy loss of the primary particle and (2) a discrete energy loss by producing delta rays. When sampling the stopping power distribution to compute the continuous energy loss of the primary particle, LArG4 uses a combination of experimental data as well as interpolation for different types of particle []. When the secondary production threshold is configured at 700 μm, the stopping power distribution of the primary particle sampled by LArG4 is experimental-based and thus, contains some smearing due to delta rays. The production of delta rays only adds some additional smearing across the dE/dx distribution.

On the other hand, when the secondary production threshold is configured at 1 μm, more energy loss is carried away by the delta rays. Isolating only energy deposition of the primary particle is equivalent to observing a *bare* proton or muon, such that the primary particle is not *dressed* with any delta rays. Experimentally, this has not been measured and therefore, the stopping power distribution of a *bare* particle is computed by LArG4 by interpolation. The rest of the energy loss and smearing is compensated by the production of delta rays. Finally, comparing between the case of proton and muon, including delta rays in the energy deposition introduces greater smearing in the dE/dx distribution for muon than that of proton.

The simulated studies demonstrate that fluctuations of delta rays can introduce two different effects to recombination. Firstly, delta rays can have a different dE/dx compared to the primary particle and therefore, can influence the effective recombination factor. At the low dE/dx spectrum of the primary particle, this results in a significant quenching of recombination whilst, at the high end of dE/dx spectrum, this can increase the observed recombination. Secondly, having a different dE/dx to the primary particle also means that delta rays can also smear the observed energy-charge scale. Finally, the magnitude of the quenching and smearing effects vary between proton and muon, suggesting a need for a particle-dependent recombination factor.

1.2.4 Impacts of Step Limits

The step limit study here aims to investigate the impacts of simulating an phenomenological model at a microphysics scale. The length dx, corresponding to the maximum distance the primary particle can travel per step, was studied at two configurable values: 0.3 mm and 3

mm. The former is the standard value employed in the simulation workflow of SBND as well as ArgoNeuT, which is one order of magnitude smaller than the wire pitch. The latter is the value of the wire pitch, which is the distance resolution observed by both detectors.

Similar analysis using the energy-charge scale was employed. The mean dQ/dx as a function of dE/dx for proton and its percentage difference to the ModBox model are plotted in Fig. **??**, for different combinations of step limits, 0.3 mm and 3 mm, and of secondary production thresholds, 700 μm and 1 μm. At the secondary production threshold of 700 μm, the increase of step limits from 0.3 to 3 mm results in an increase of the effective recombination factor across the whole range of dE/dx. The largest magnitude of increase is between the range dE/dx from 2 to 8 MeV/cm, where the majority of energy deposition occurs, and reduces with higher value of dE/dx. On the other hand, at the secondary production threshold of 1 μm, the effect from varying the step limit is insignificant. The step limit increase affects the primary particle more than the delta rays. This is due to the track length of the primary particle is significantly longer than that of delta rays, and therefore, more likely to propagate with step length up to 3 mm.

This result demonstrates even though the effective recombination model was simulated at the observed wire pitch distance of 3 mm, the simulation result might not return the same energy-charge scale. This is due to the fact that the ArgoNeuT parameters were tuned using the simulation with the step length dx configured at 0.3 mm, one order of magnitude less than the wire pitch. Therefore, the simulation workflow of SBND only shows a good agreement when using the same configuration as ArgoNeuT. This shows a strong inter-

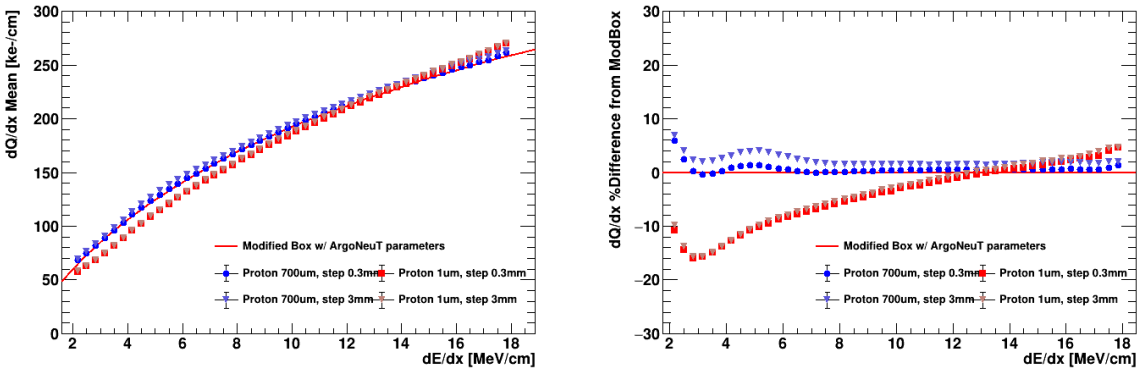

(a) **(b)**

Fig. 1.8 Plots of the mean dQ/dx (left) and its percentage difference relative to the ModBox model (right) as a function of dE/dx for a 1 GeV proton, at secondary production thresholds of 700 μm and 1 μm and at step limits of 0.3 mm and 3 mm.

dependency between the detector simulation and experimental data, particularly when it comes to tuning a phenomenological parameter for a simulation workflow.

1.2.5 Concluding Remarks

The simulated study shows that fluctuations in delta rays can influence the recombination factor. A similar simulation-data comparison study of recombination was carried by the ICARUS collaboration [3]. The result is shown in Fig. **??**, showing a quenching effect at both low and high values of secondary production thresholds. The experiment proposed a few different approaches towards recombination simulation. The first approach is to simulate *as microscopic as possible*, by generating low energy delta rays with kinetic energy as low as 1 eV and range of order tens of nm. However, this does not work for two reasons that have been previously stated and verified in this study. Firstly, the recombination measured in data is of a particle *dressed* in delta rays and secondly, limited computing resource constraints generating and tracking delta rays in that order of magnitude. Another proposal was an empirical approach, by choosing the best secondary production threshold in simulation to reproduce the data. This number was found to be 3 μm, equivalent to delta rays having kinetic energy of 10 keV.

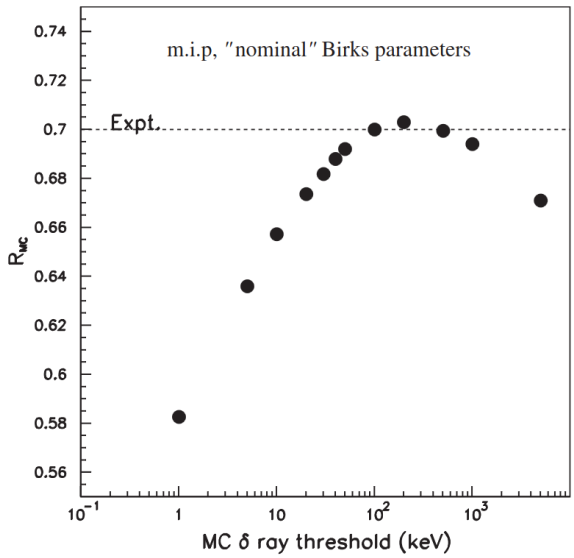

Fig. 1.9 The simulated recombination factor as a function of the secondary production threshold as carried out by the ICARUS collaboration. The dotted line is the measured recombination factor using Birks formalism. Fig. from [3].

Since this simulated study was carried in 2021, understanding and modelling of recombination has been greatly improved. Notably, recent results from ICARUS experiment [] has demonstrated a clear dependence of recombination on the angle of the ionising particle track to the drift electric field. An ellipsoid modified box model of recombination was proposed and able to describe the data across all measured angles. There still remains a lot of work to enhance our current understanding of recombination. In the scope of calibrating the SBND detector, it is highly recommended to follow a data-driven approach such that the simulation should be tuned to best match the observed data, as it has been done by earlier experiments like ICARUS and ArgoNeuT. This simulated study demonstrates a strong inter-dependency between detector simulation and data and therefore, the accuracy of recombination factor can be improved by using parameters tuned to data measured by SBND. Moreover, the study shows a distinct difference in recombination between proton and muon and suggests a need for particle-dependent model. Modelling recombination for a specific sample of particle type is feasible with the large statistics of SBND. This will allow for constructing a particle-dependent recombination factor and therefore, allowing quick computation of the factor and its associated smearing per propagation step LArG4. This data-driven recommendation aims to improve the accuracy of the recombination simulation without exhausting commutating resource.

References

[1] R. Acciarri et al., "A study of electron recombination using highly ionizing particles in the argoneut liquid argon tpc", Journal of Instrumentation **8**, P08005 (2013).

[2] M. Szydagis et al., "A Review of Basic Energy Reconstruction Techniques in Liquid Xenon and Argon Detectors for Dark Matter and Neutrino Physics Using NEST", Instruments **5**, 13 (2021).

[3] S. Amoruso et al., "Study of electron recombination in liquid argon with the icarus tpc", Nuclear Instruments and Methods in Physics Research Section A: Accelerators, Spectrometers, Detectors and Associated Equipment **523**, 275–286 (2004).